


Cite this: *Mater. Adv.*, 2023,  
4, 3662Received 16th June 2023,  
Accepted 17th July 2023

DOI: 10.1039/d3ma00309d

rsc.li/materials-advances

## Electrodeposition, composition and properties of cobalt–rhenium alloys coatings

Yuliya Yapontseva,<sup>a</sup> Valeriy Kublanovsky,<sup>b</sup>  <sup>✉</sup> Tetyana Maltseva,<sup>a</sup>  
Yuri Troshchenkov<sup>b</sup> and Oleksii Vyshnevskiy<sup>c</sup>

This paper compares the chemical composition, current efficiency, crystal structure, as well as the magnetic, electrocatalytic, and corrosion properties of CoRe electrolytic alloys deposited from alkaline electrolytes of two complex compositions: monoligand citrate and polyligand citrate pyrophosphate ones. It is shown that with the deposition of alloys from citrate electrolytes it is possible to obtain X-ray amorphous coatings with high rhenium content (up to 78 at% of Re). In a citrate–pyrophosphate electrolyte, the electroreduction of cobalt proceeds with a low overvoltage, so the proportion of rhenium in the coating decreases sharply (to 12 at% of Re); and the coatings are formed with a crystalline structure. Changing the ratio of alloy components in a wide range makes it possible to obtain both non-magnetic coatings and ferromagnetic ones. The relationship between the electrocatalytic properties of alloys in the hydrogen evolution reaction and the corrosion resistance of coatings in an alkaline medium is found in a wide range of rhenium concentrations, in which it cannot be traced for electrolytic alloys of other refractory metals (Mo and W) due to the impossibility of obtaining alloys containing more than 35 at% of molybdenum or tungsten.

## Introduction

The increased interest of researchers towards the electrolytic rhenium alloys in recent years is associated with the need for mechanical engineering and the aerospace industry for materials with increased strength characteristics, as well as the search for effective electrocatalytic materials for many processes based on non-platinum metals. The quality, structure and chemical composition of electroplated coatings are directly determined by the quantitative and complex composition of electrolytes, as well as the electrolysis mode. Since rhenium is released from aqueous solutions only in the form of a polyoxide system,<sup>1</sup> but quite easily forms electrolytic alloys with iron group metals (in our case, with cobalt),<sup>2,3</sup> the electrodeposition of such an alloy is directly related to the overvoltage of cobalt release from complex compounds of its ions in electrolyte solution. Electrolytic rhenium and alloys of rhenium with metals of the iron subgroup can also be obtained from water-in-salt type electrolytes.<sup>4–6</sup> However, a high-quality coating without cracks in this case can be obtained only at a thickness of 200–300 nm

in the potentiostatic mode, and the coating of micron thickness is destroyed during storage. Crystal hydrate electrolytes of this type cannot be considered aqueous in the commonly used sense. The mechanism of the formation of electrolytic alloys in them has been less studied and should be fundamentally different from the electroreduction of metals from aqueous complex solutions with parallel hydrogen evolution. To obtain coatings with a thickness of 1–10 μm, aqueous electrolytes are the most promising. The use of solutions of various complex compositions<sup>7–9</sup> leads to the formation of alloys with a rhenium content in a very wide range, which implies a wide variety of surface functional properties that can be obtained by electroplating.

As shown in ref. 2 and 10, high-quality coatings with a rhenium content of 45–65 at% can be obtained by electrodeposition from a citrate (Cit) electrolyte at pH 3.5. It is known that the composition and properties of electroplated coatings depend on the composition of electrochemically active complexes, *i.e.* on the composition of ions that react directly on the electrode surface, and the discharge of which at the cathode leads to the formation of a metal or alloy. The number, concentration and composition of electrochemically active complexes, in turn, depend on the pH of solution. In a citrate solution, taking into account the theoretical possibility of substituting four protons in a citric acid molecule, at low pH values the simultaneous existence of several protonated forms of cobalt citrate,<sup>11</sup> as well as the citrate complex of rhenium is possible.<sup>12</sup> At a pH value of 3.5, the highest concentration in the

<sup>a</sup> V. I. Vernadsky Institute of General and Inorganic Chemistry NAS of Ukraine, Akad. Palladina Ave 32/34, 03142 Kyiv, Ukraine. E-mail: kublan@ukr.net<sup>b</sup> Institute of Magnetism NAS of Ukrainian and MES of Ukraine, Akad. Vernads'koho Blvd. 36-b, 03142, Kyiv, Ukraine<sup>c</sup> M.P. Semenenko Institute of Geochemistry, Mineralogy and Ore Formation NAS of Ukraine, Akad. Palladina Ave 34, 03142 Kyiv, Ukraine

solution is observed for the  $\text{H}_2\text{CoCit}$  and  $\text{HCoCit}^-$  complexes, which can be discharged at the cathode to form metal cobalt. If we take into account the fact that, during electrolysis, the pH of the near-electrode layer shifts significantly to the alkaline region, then the probability of participation of the  $\text{H}_2\text{CoCit}$  complex in the electrodeposition process becomes negligibly small, and the most probable complex form that predetermines the discharge remains  $\text{HCoCit}^-$ .

During the electrodeposition of a binary CoRe alloy from an electrolyte with pH 3.5,<sup>2</sup> we have shown the possibility of reducing rhenium to a metal due to ad-atoms of hydrogen, which are formed as a result of a parallel cathodic reaction of hydrogen evolution. Since there are many proton donors in an acidic environment, including both protonated cobalt citrate complexes and protonated citrate ions, which are in excess, the idea of precipitating a binary alloy from a solution, in which water will remain practically the only donor of protons, arose, and the formation of metals will occur from non-protonated complex compounds. Therefore, we carried out the deposition of coatings from a citrate electrolyte with a pH of 9.0. In such a solution (especially if alkalization of the near-cathode layer is taken into account), only non-protonated cobalt complexes and bimetallic complex compounds based on them are electroactive. So it should be possible to influence the chemical composition of alloys due to the change in some electrodeposition conditions in comparison to that reported in Ref. 2.

Let us now consider the effect of adding a second complexing agent to electrolyte, namely, potassium pyrophosphate. As it is known, during the electrodeposition of cobalt with other refractory metals, for example, with molybdenum, an acidic citrate electrolyte makes it possible to obtain high-quality, uniform and finely crystalline coatings, but with a low current efficiency<sup>13</sup> due to a large overvoltage of metal deposition, and an alkaline pyrophosphate electrolyte (PPI) has a high current efficiency, but the coatings are very stressed and hydrogenated and have poor adhesion to the surface.<sup>14</sup> The mixed citrate–pyrophosphate (Cit–Ppi) electrolyte overcomes the disadvantages of both of these solutions. The presence of pyrophosphate ions in the solution makes it possible to form an alloy by a mechanism,<sup>15</sup> not by the generally accepted mechanism of induced coprecipitation, which includes the stage of formation of bimetallic citrate complexes in the bulk of the solution<sup>7</sup> or on the cathode surface immediately before the discharge.<sup>16</sup> Besides, cobalt can be reduced from a polyligand complex of composition  $\text{Co}(\text{Cit})(\text{Ppi})$ .<sup>17</sup>

The aim of this article was to compare the chemical composition and properties of CoRe coatings deposited from a monoligand citrate electrolyte with low and high pH values, as well as from a polyligand citrate pyrophosphate electrolyte.

## Experimental section

### Materials and methods

The electrodeposition of CoRe alloys was carried out from citrate and citrate–pyrophosphate electrolytes, the composition of which is presented in Table 1.

**Table 1** The composition of electrolytes for the deposition of CoRe alloys ( $\text{mol L}^{-1}$ )

Electrolyte	$\text{CoSO}_4$	$\text{KReO}_4$	$\text{Na}_3\text{C}_6\text{H}_5\text{O}_7$	$\text{K}_4\text{P}_2\text{O}_7$	$\text{Na}_2\text{SO}_4$
#1 (Cit)	0.1	0.01	0.2	—	0.3
#2 (Cit–PPI)	0.1	0.01	0.2	0.2	0.3

pH value of electrolytes – 9.0.

The studies were carried out under conditions of both natural convection and intensive mixing at a rotation speed of a magnetic stirrer of 300 rpm in a thermostated cell at a temperature of 50 °C in a galvanostatic mode using a direct current source LIPS-35 in the current density range of 5–40  $\text{mA cm}^{-2}$ , a copper plate with an area of 1  $\text{cm}^2$  was used as a working electrode, and the anode was platinum. The electrodeposition time is 1 hour for current densities of 10–40  $\text{mA cm}^{-2}$  and 2 hours for a current density of 5  $\text{mA cm}^{-2}$ .

The thickness of the coatings was calculated based on the weight gain of the sample after deposition, the chemical composition of the alloy (wt%) and the density of each of the metals using the formula:

$$\delta = \frac{m_{\text{alloy}}}{\rho_{\text{alloy}} \times S} = \frac{m_{\text{alloy}}}{(\rho_{\text{Co}} \times \text{wt}\%_{\text{Co}} + \rho_{\text{Re}} \times \text{wt}\%_{\text{Re}}) \times S}$$

where  $\rho_{\text{Co}}$  and  $\rho_{\text{Re}}$  are the density values of cobalt and rhenium, respectively; wt% is the mass fraction of cobalt and rhenium, respectively;  $m_{\text{alloy}}$  is the weight of the alloy;  $S$  is the area of the electrode.

The calculated coating thickness for electrolyte #1 was 2.5–3.5  $\mu\text{m}$ ; for electrolyte #2 4–7.5  $\mu\text{m}$  depending on the deposition current density.

### SEM and EMPA

The morphology and chemical composition of samples were studied by using a JSM-6700F field emission scanning electron microscope equipped with a JED-2300 energy-dispersive spectrometer (JEOL). The operating conditions were as follows: 20 kV accelerating voltage, 0.75 nA beam current, and 1  $\mu\text{m}$  beam size. The counting time for EDS analyses was 60 s. Pure Co and Re were used as standards. The raw counts (Co, K $\alpha$ ; Re, L $\alpha$ ) were corrected for matrix effects with a ZAF algorithm implemented by JEOL. Three to five spots per each sample were analyzed.

### X-ray phase analysis

The X-ray patterns were recorded on a diffractometer (DRON-3.0) with Bragg–Brentano geometry and using Cu-K radiation ( $= 1.54183 \text{ \AA}$ ), which operates at 30 kV and 30 mA at a constant scan rate of 0.02–2  $\text{s}^{-1}$ .

### Magnetic measurement

The magnetic properties of the deposits obtained were determined using a magnetometer with a vibrating sample in fields up to 20 kOe at room temperature.



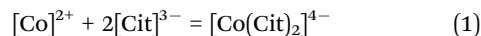
## Corrosion studies

The study of corrosion was carried out by voltammetry. These measurements were carried out using an MTech PGP-550F potentiostat-galvanostat<sup>18</sup> in a 1 M KOH solution at a temperature of  $20 \pm 1$  °C in a cell assembled according to a three-electrode circuit with a silver reference electrode and an auxiliary electrode, which is a platinum grid. Voltammetric studies of corrosion consisted of obtaining cathodic and anodic polarization curves with a potential sweep rate of  $1.0 \text{ mV s}^{-1}$ . As a result of the analysis of polarization measurements in the region of stationary potential ( $\pm 100 \text{ mV}$ ), the corrosion resistance was calculated.

## Results and discussion

In Fig. 1 is shown the content of rhenium in binary alloys depending on the current density for all of the deposition electrolytes. Dependence (1) is taken from ref. 2 The figure shows that an increase of the pH value of the citrate electrolyte leads to an increase in the rhenium content in the alloys by an average of 20 at% at all current densities applied. It is known that electrolytes containing complexing agents are used to increase the metal deposition overvoltage in order to obtain a more finely crystalline deposit as well as to shift the metal deposition potentials to their convergence for the formation of an electrolytic alloy. In our case, with a twofold excess of citrate ions, on the one hand, the non-protonated cobalt citrate complex  $[\text{Co}(\text{Cit})_2]^{4-}$ <sup>19,20</sup> is formed in the solution in accordance with eqn (1). The authors of ref. 21 showed that with an increase in the pH of an electrolyte containing a twofold excess of citrate ions, the cobalt release potential shifts to the negative side, and at  $\text{pH} > 8$  the hydrogen release potential is reached earlier than the metal deposition potential. In this case, only hydrogen evolution occurs at the cathode, and even at high current densities, it is not possible to obtain a metal deposit in

an amount sufficient to determine the current efficiency by the gravimetric method.



On the other hand, the solution contains rhenium, which at pH 9.0 exists as a perrhenate ion and is not bound into strong chemical compounds that could make it difficult for electro-deposition; nevertheless, the electroreduction of the perrhenate ion leads to the formation of a thin film of rhenium oxides in the same way as was shown by the authors.<sup>22</sup>

In fact, neither cobalt nor rhenium can be deposited as a solid metal coating separately from an alkaline solution with a twofold excess of ligand. Nevertheless, there is a synergistic effect of the components and the formation of an electrolytic alloy, which cannot be explained by the formation of bimetallic complex compounds in solution, but the formation of electro-active particles on the cathode surface is possible immediately after the adsorption of metal-containing compounds.

The addition of pyrophosphate ions to the ratio  $\text{Co}:\text{Cit}:\text{PPI} = 1:2:2$  leads to the formation of a polyligand complex  $[\text{Co}(\text{PPI})\text{Cit}]^{5-}$  according to reaction (2).<sup>17</sup> Electroreduction of this complex leads to a sharp increase in the cobalt content in the alloy up to 77–87 at%, as seen in Fig. 1, curve 3.



In contrast to the acidic citrate electrolyte, where rhenium, not cobalt, is predominantly reduced at the cathode<sup>2,23</sup> despite the low concentration of its ions in solution, the use of Cit–PPI electrolyte and varying the ligand ratio makes it possible to accurately select the coating composition within a wide range, and make it possible to solve a various specific technical problem. In general, the different ratio of refractory, hard and wear-resistant rhenium and ferromagnetic cobalt, in turn, gives a wide range of possible applications as a coating for hardening the surface of products, increasing the electrocatalytic activity of electrodes, or for imparting magnetic properties to the surface.

Fig. 2(a) shows the fundamental difference between the dependences of the current efficiency on the deposition current density for alloys deposited from electrolytes with different pH values. So, for an acid electrolyte, this dependence has a minimum at  $10 \text{ mA cm}^{-2}$ , and in alkaline electrolytes, the value of the current efficiency is constantly decreasing. For both alkaline solutions, the total dependences are very similar; however, the partial fractions of each of the elements are significantly different. It can be seen from Fig. 2(b) that the difference is significant not only at different pH values, but also at different complex compositions of solutions.

Thus, in citrate electrolytes, rhenium contributes the main share in the current efficiency, and in Cit–PPI electrolyte, cobalt is the main contribution. It should be noted that the partial current efficiency of cobalt and rhenium deposition in the Cit–PPI electrolyte has very close values, *i.e.*, the metals are reduced at approximately the same rate, if can it be converted to the partial deposition current density.

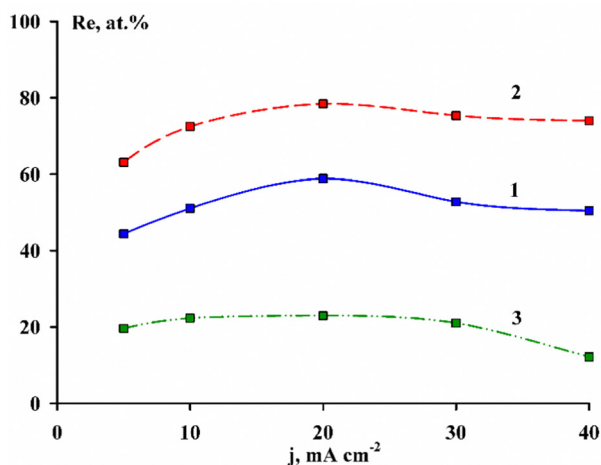


Fig. 1 Dependence of the rhenium content in CoRe alloys on the current density during deposition from Cit electrolyte at pH 3.5 (1)<sup>2</sup> and 9.0 (2) and Cit–PPI electrolyte (3).



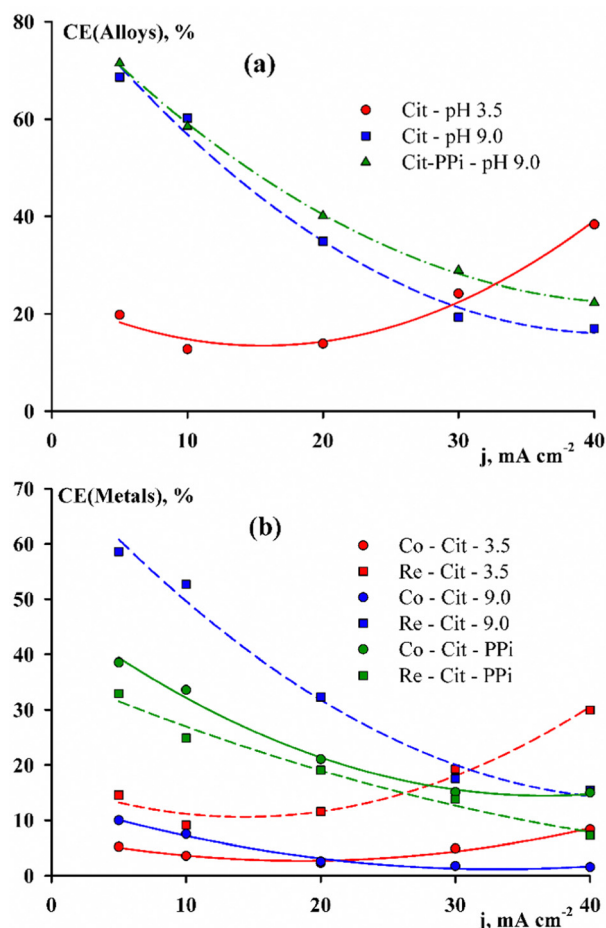


Fig. 2 Current efficiency of CoRe alloys deposited from various electrolytes (a) and the partial current efficiency for each of the metals (b).

Fig. 3 shows that the complex composition of the deposition electrolytes has a decisive influence not only on the chemical composition, but also on the surface morphology of the resulting alloys. Coatings obtained from Cit-PPI electrolyte have significant internal stresses and crack, which is also characteristic of alloys of other refractory metals.<sup>24</sup>

Based on the smooth edges of the cracks, it can be concluded that they were formed not during the electrodeposition process, but after the current was switched off. This behavior is associated with the ability of rhenium for hydrogenation. It could be expected that the more rhenium in the coating, the greater the amount of absorbed hydrogen and the greater the internal stresses; and that is true when hydrogen is formed on an already formed coating during electrolysis in a KOH solution, but in the process of electrodeposition and formation of a crystal lattice, parallel formation of hydrogen atoms leads to the opposite effect. This is due to the electrocatalytic properties of CoRe alloys in the reaction of hydrogen evolution in alkaline media. Using ternary alloys as an example, we have shown in ref. 25 and 10 that the amount of refractory metals (including rhenium) in the alloy up to 30 at% contributes to an increase in the current density of hydrogen exchange during evolution in KOH solution compared to pure cobalt. The higher

the rate of formation of hydrogen *ad*-atoms on the surface, the greater the probability of their diffusion into the metal crystal lattice, and this process contributes to hydrogenation and an increase in internal stresses.

Fig. 3(d)–(f) show an increase in cracks with an increase in the deposition current density, which corresponds to a decrease in the overvoltage of hydrogen evolution on these alloys and also explains the significant decrease in the current efficiency of the alloys during their deposition and, accordingly, an increase in the rate of the parallel reaction of hydrogen evolution.

Fig. 4 shows X-ray diffraction patterns of alloys deposited from Cit and Cit-PPI electrolytes on the same scale. There is disagreement in the modern literature as to whether a material with a broad diffuse diffraction peak should be called X-ray amorphous<sup>26</sup> or nanocrystalline.<sup>27</sup> In addition, it has been suggested that for electrolytic alloys of refractory metals, the simultaneous existence of intermetallic and solid solution phases is possible. Moreover, one of these phases can be nanocrystalline, and the other amorphous. This conclusion<sup>27</sup> was made on the basis of the calculated parameters of the unit cell. From the size of the broad peak, which in terms of the diffraction angle corresponds to a solid solution of rhenium in cobalt, as well as the formation of the intermetallic compound Co<sub>0.8</sub>Re<sub>0.2</sub>, one can approximately estimate the crystallite size of 2–3 nm. It should be noted that for the same amount of electricity passed when depositing samples from different electrolytes, the current efficiency of electrodeposition of an alloy from a citrate solution is low and the coatings have a thinner thickness than those deposited from Cit-PPI electrolyte. Therefore, clear peaks of the copper substrate are visible in the figure. It can be seen from Fig. 4(b) that the use of a polyligand deposition electrolyte radically changes not only the ratio of elements in the alloy and the current efficiency, but also the size of the formed crystallites.

The crystallite size was estimated from the peak width and angular position using the Scherrer's equation:

$$d = \frac{0.9\lambda}{b \cos \theta} \quad (3)$$

where  $d$  is the size of crystallites (nm);  $\lambda$  is the wavelength of copper radiation (nm);  $b$  is the peak half-width;  $\theta$  is the diffraction angle.

The sizes of crystallites calculated by eqn (3) are shown in Fig. 5. It can be seen that with an increase in the deposition current density within the range 5–40 mA cm<sup>-2</sup>, a transition occurs from the crystalline structure of the coatings to an amorphous one. In this case, the largest crystallite size is observed at 10 mA cm<sup>-2</sup> and it is 57 nm.

The formation of a textured coating is associated primarily with the amount of cobalt. For example, an hcp crystal structure with a predominant (002) orientation was obtained for pure electrolytic cobalt.<sup>28</sup> Similar results were obtained with an increase in the cobalt content in the alloy with an increase in the deposition current density for ternary CoWRe alloys in ref. 25.





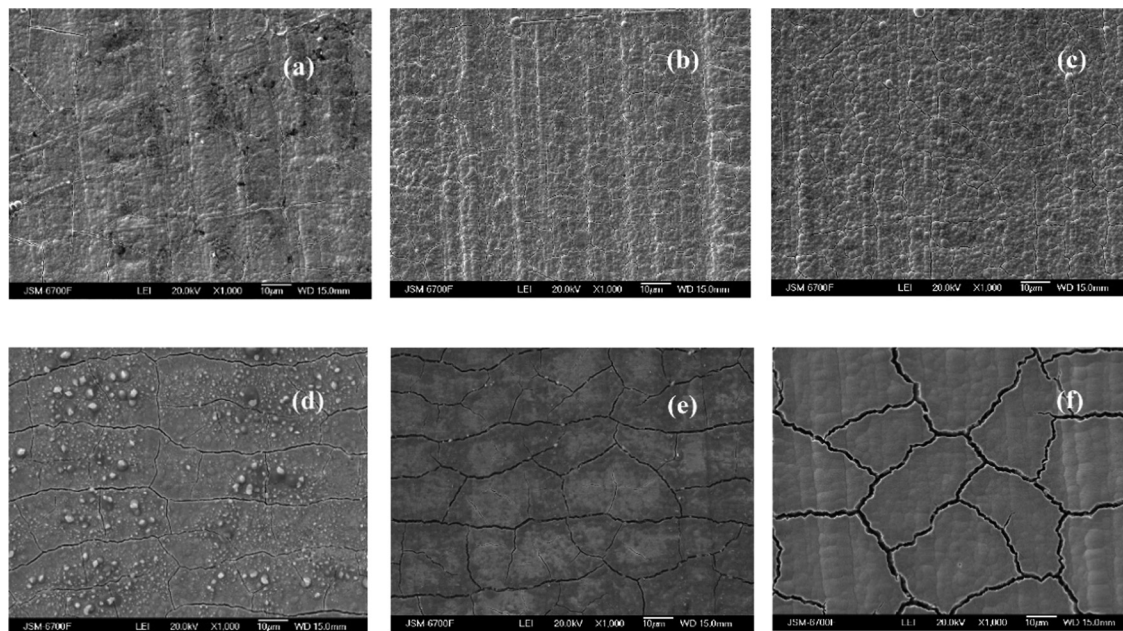


Fig. 3 Surface morphology of CoRe alloys deposited from Cit (a)–(c) and Cit–PPI (d)–(f) electrolytes at the deposition current density,  $\text{mA cm}^{-2}$ : 5 – (a), (d); 10 – (b), (e); 30 – (c), (f).

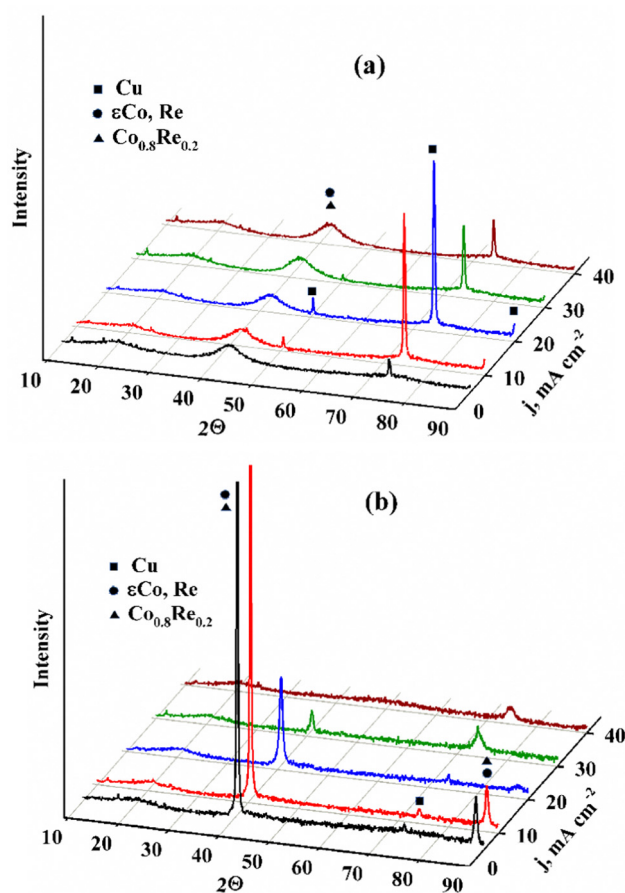


Fig. 4 XRD of alloy coatings deposited at current densities 5–40  $\text{mA cm}^{-2}$  from electrolytes No 1 (a); No 2 (b).

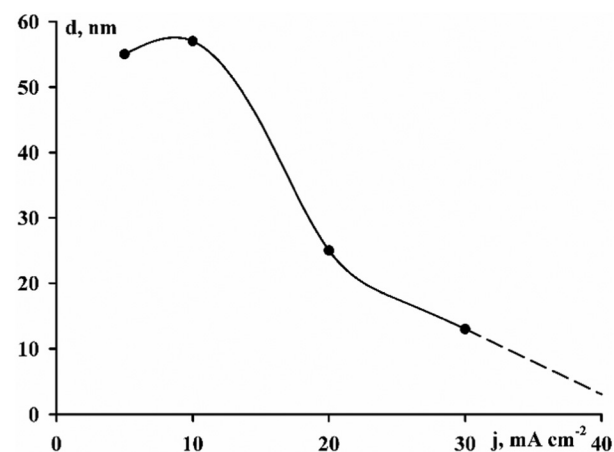


Fig. 5 Dependence of the crystallite size on the deposition current density.

All coatings obtained from Cit electrolyte are not magnetic at room temperature due to the low content of the ferromagnetic component, *i.e.* cobalt. Therefore, studies of the magnetic properties were carried out only for coatings deposited from Cit–PPI electrolyte.

As can be seen from Fig. 6, coatings deposited at different current densities differ significantly in their magnetic properties. The magnetic hysteresis parameters are given as a function of the deposition current density, despite the fact that there is no direct unambiguous relationship between the technological parameter during deposition and the properties of the final product. Current density is a factor that simultaneously affects



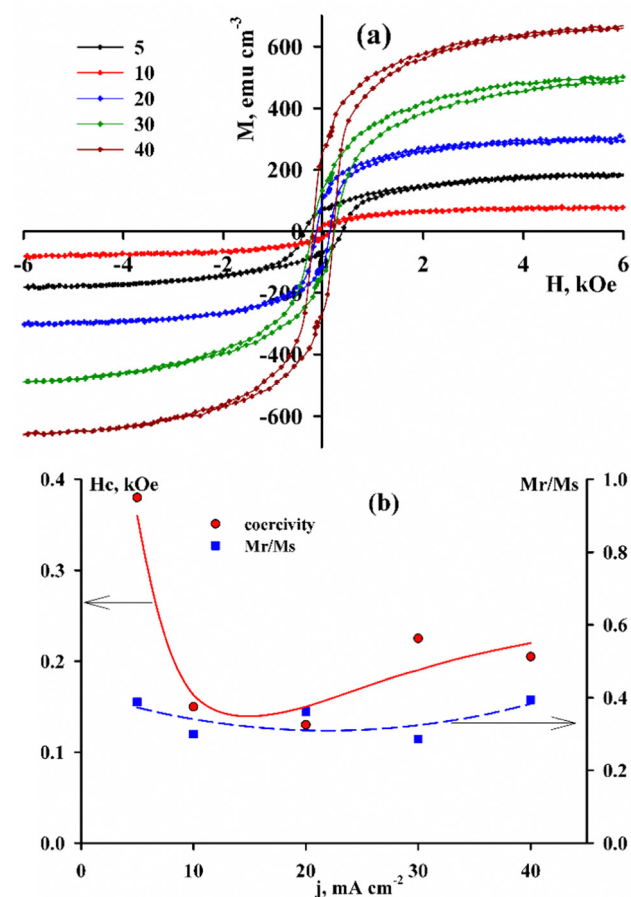


Fig. 6 Magnetic hysteresis loops (a) and loop parameters (b) of CoRe alloys (the deposition current density is shown in the figure).

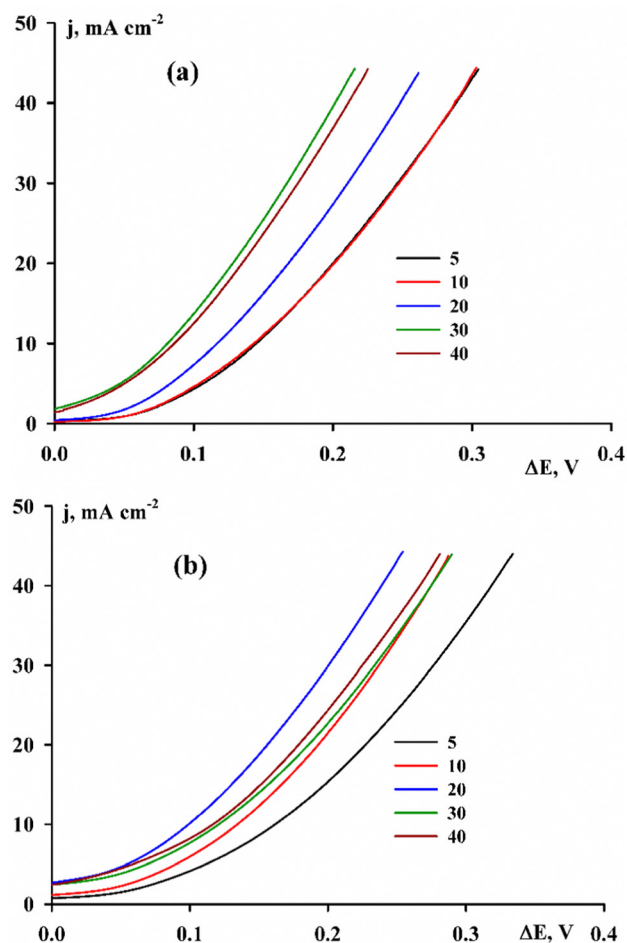


Fig. 7 Current–voltage curves of hydrogen evolution in a 1 M KOH solution on alloys deposited from Cit (a) and Cit–PPI (b) electrolytes.

the chemical composition and structure of coating, and thus determines the properties of alloys.

Taking into account that the chemical composition of the alloys in this case varies insignificantly, and it can be assumed that the crystal structure is a factor that determines the parameters of the magnetic hysteresis. Thus, the saturation magnetization ( $M_s$ ) during the transition from the crystalline structure to the amorphous one increases by more than 10 times. The coercive force varies over a wide range from 130 to 380 Oe. At the same time, the squareness coefficient of the loop remains at the level of 0.35–0.4, which puts these coatings in an intermediate position between soft and hard magnetic materials.

Another important property of electrolytic rhenium alloys is the electrocatalytic activity in the hydrogen evolution reaction. In Fig. 7 it is shown that the activity of the alloys increases with increasing the deposition current density.

The main criteria for evaluating electrocatalytic activity are the exchange current of hydrogen  $j_0$  and the overvoltage of the hydrogen evolution reaction (HER)  $\Delta E$ . The coefficients of the Tafel equation were calculated directly from the experimental voltammetric measurements, not only to calculate the exchange current density, but also to determine the mechanism of hydrogen evolution on the surface under study based on the

value of the Tafel slope  $b$ . In the case of pure electrolytic cobalt, the coefficients of the Tafel equation are:  $a = 0.49$  V,  $b = 0.120$  V,  $-\log j_0 = 4.08$  A cm<sup>-2</sup>, and  $\Delta E_{10} = 0.250$  V (overvoltage at a current density of 10 mA cm<sup>-2</sup>).<sup>25</sup>

On all coatings with alloys, the value of the exchange current density  $j_0$  is higher, and the hydrogen evolution overvoltage is lower, *i.e.*, the alloy is a better electrocatalyst than cobalt. For the alloys deposited from the Cit electrolyte, the value of  $-\log j_0$  is within the range of 2.73–3.75, and the value of  $\Delta E_{10} = 80$ –145 mV. Both indicators decrease with the increase of deposition current density. Taking into account that the chemical composition varies within a small range, the experimentally obtained increase in catalytic activity can be associated with an increase in the true surface area compared to the geometric one under conditions of both rapid growth of the deposit and the growth of hydrogen bubbles. For alloys containing a smaller amount of rhenium (deposited from Cit–PPI electrolyte), the logarithm of the exchange current density and the overvoltage of hydrogen evolution are  $-\log j_0 = 2.6$ –3.2 and  $\Delta E_{10} = 100$ –160 mV, respectively. It could be assumed that the properties of the alloys do not depend on a large or small amount of rhenium, and only the presence of rhenium atoms



on the surface is sufficient to improve the electrocatalytic activity compared to pure cobalt. However, when comparing the properties of the coatings obtained from all the solutions studied, a clear dependence of the parameters of the hydrogen evolution reaction on the ratio of elements on the electrode surface can be traced.

Electrodeposition of CoRe alloys from solutions containing various Co(II) complexes makes it possible to obtain coatings within a wide range of rhenium content (Fig. 8), in contrast to electrolytic alloys of other refractory metals (molybdenum and tungsten). Therefore, it is possible to trace the change in kinetic parameters, which is impossible for other coatings with similar electrocatalytic properties. For alloys obtained from different electrolytes, *i.e.*, with different ratios of components, the difference in Tafel slopes is obvious. So for coatings with a high content of rhenium, the values of coefficient *b* are within the range of 70–110 mV, for coatings with a low content of rhenium – 115–170 mV, and for alloys with a ratio of cobalt and rhenium of approximately 1:1 – 64–73 mV. In this case, we are not talking about a change in the reaction mechanism, but rather a change in the properties of the surface, as was shown in,<sup>25</sup> and it is related to the degree of filling of the surface with both metal atoms: atoms of refractory metal, on which the stage of electron transfer (Volmer reaction) occurs quickly and reversibly, and with metal atoms of the iron group, on which the stage of electrochemical desorption occurs quickly and reversibly (the Heyrovsky reaction). Fig. 8 shows that the dependence of the coefficient *b* has a minimum at the ratio Co:Re = 1:1, which indirectly confirms the hypothesis that the Volmer reactions (*b* = 120 mV is a characteristic value for the rate-determining stage for metals of the iron group) and Heyrovsky (*b* = 40 mV is a characteristic value for the rate-determining stage on metals such as platinum) can pass at comparable speeds. Under the conditions of our experiment, alloys with a rhenium content within the range of 25–40 at% were not obtained.

Nevertheless, the literature data on the electrocatalytic activity of alloys of other refractory metals in the reaction of

hydrogen evolution in an alkaline medium confirm the form of the dependence for the coefficient *b* shown in Fig. 8 precisely for this range of refractory metal concentration. Thus, in<sup>29</sup> for CoMo alloy containing 33 at% Mo *b* = 83 mV dec<sup>−1</sup>, for CoMoP – *b* = 63–77 mV dec<sup>−1</sup>,<sup>30</sup> for CoMo coating containing Mo 11–40 wt% *b* varies within the range of 109–96 mV dec<sup>−1</sup>,<sup>31</sup> as well as for tungsten alloys with a content of 5–33 wt% W *b* = 184–146).<sup>32</sup>

In accordance with the value of *b*, the calculated exchange current density changes. Based on the dependence of  $-\log j_0$  on the amount of rhenium (Fig. 8), coatings with a low content of refractory metals (10–20 at%) or with a high content (70–80 at%) will have the best electrocatalytic properties. Since the values of coefficient *b* differ significantly for alloys of different compositions, the comparison of the exchange current calculated with their usage is only a rough estimate. The most adequate criterion for evaluating the electrocatalytic activity in this case is the overvoltage of the HER at the same selected current density. In our case a comparison at current densities of 10 and 40 mA cm<sup>−2</sup> was chosen ( $\Delta E_{10}$ ,  $\Delta E_{40}$ ). In Fig. 8 it is shown that at a low current density (10 mA cm<sup>−2</sup>) the overvoltage value decreases monotonically with an increase in the rhenium content in the alloy; the dependence at higher current densities (40 mA cm<sup>−2</sup>) can be interpreted as having a small minimum or stabilization at approximately the same level at a rhenium content of  $\geq 50$  at%. Taking into account all the calculated parameters, coatings containing 60–70 at% rhenium have the highest exchange current at the lowest HER overvoltage, and to obtain it, it is necessary to use citrate monoligand electrolytes.

Since electrolytic hydrogen, as a rule, is obtained in concentrated alkaline solutions, information about the corrosion resistance in such media for coatings with alloys of refractory metals<sup>33</sup> as promising materials for HER electrocatalysis is needed.

The results of corrosion studies (Fig. 9) show that there is a relationship between corrosion resistance and rhenium content in alloys, the minimum of which falls on coatings containing 50–60 at% rhenium.

The electrocatalytic properties of the surface of alloys in alkaline medium are manifested in all cases: when hydrogen is the target product and when hydrogen evolution is an integral part of the corrosion process. In the absence of oxygen access to the surface of the corroding metal, the process proceeds with hydrogen depolarization. Taking into account the best conditions for electrocatalysis indicated above, *i.e.*, the minimum overvoltage of the HER in combination with an increasing exchange current, alloys with a rhenium content of  $\approx 60$  at% show the highest rate of hydrogen reduction as a depolarizer. If the rates of oxidation and reduction reactions are equal, the corrosion of this metal under such conditions will be the greatest.

The value of corrosion resistance of coatings at very low concentrations of rhenium on the one hand and high concentrations of rhenium on the other hand approaches the corrosion characteristics of pure metals cobalt and rhenium, respectively. The corrosion of electrolytic cobalt in an alkaline medium is given in<sup>34</sup> and, according to the data of impedance spectroscopy, is 1.9 kΩ cm<sup>2</sup>, which fully corresponds to the

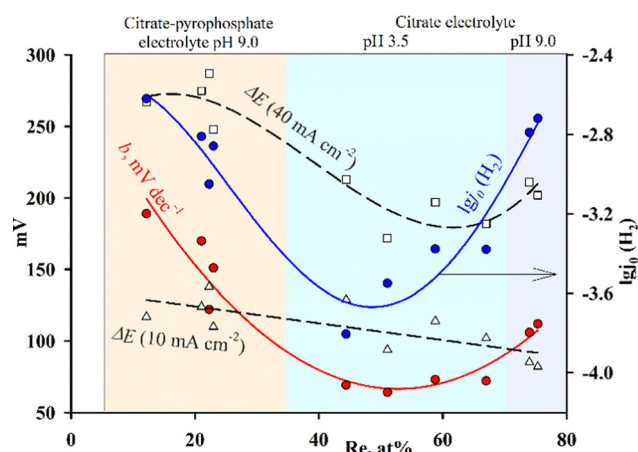


Fig. 8 Dependences of the kinetic parameters of the reaction of hydrogen evolution on the content of rhenium in the alloys; the values for the alloys deposited from Cit electrolyte at pH 3.5 are taken from.<sup>2</sup>





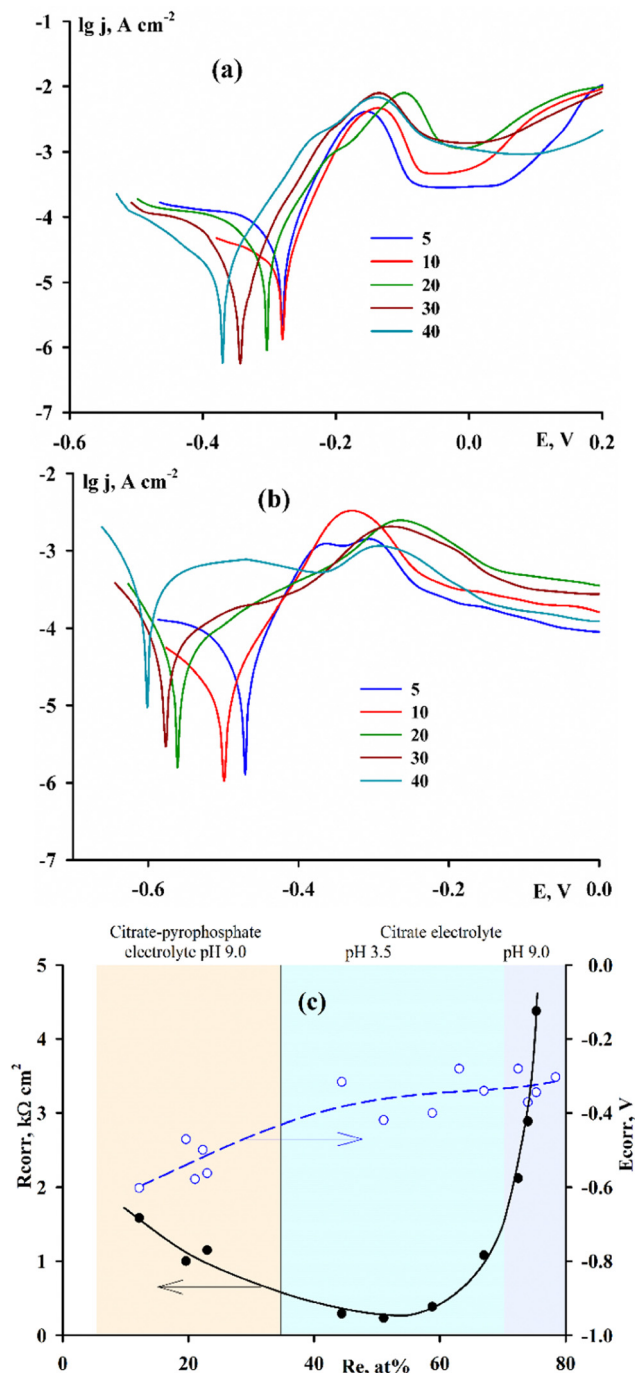


Fig. 9 Current–voltage curves of corrosion in a 1 M KOH solution of alloys deposited from Cit (a) and Cit–PPi (b) electrolytes; the dependence of resistance and corrosion potential on the content of rhenium in alloys (c).

dependence in Fig. 9, and rhenium is indicated in ref. 35 as one of the very stable metals in alkaline medium.

## Conclusions

– Comparison of the chemical composition of CoRe coatings deposited from a monoligand citrate electrolyte with low and high pH values, as well as from a polyligand citrate

pyrophosphate electrolyte showed that it is possible to obtain coatings with high rhenium content only from citrate electrolytes. This is due to the fact that in the citrate–pyrophosphate electrolyte, the process of electroreduction of cobalt proceeds with a low overvoltage and the proportion of cobalt in the coating increases sharply.

– Significant differences in the ratio of alloy components lead to the formation of coatings of various structures: X-ray amorphous and crystalline.

– Changing the amount of ferromagnetic cobalt in the alloy within a wide range makes it possible to obtain coatings that are not magnetic or have magnetic properties.

– Interrelation of electrocatalytic, corrosion properties of coatings depending on the content of rhenium in alloys is revealed. And coatings containing 60–70 at% rhenium have the highest exchange current at the lowest HER overvoltage.

– The presence of electrocatalytic properties in coatings contributes to the release of hydrogen during corrosion with hydrogen depolarization, which leads to a decrease in the corrosion resistance of alloys in an alkaline environment.

– Coatings with CoRe alloys have strong electrocatalytic properties in the reaction of hydrogen evolution. To determine the optimal composition of the electrocatalyst, it is necessary to simultaneously fulfill two main conditions: a low hydrogen evolution overvoltage and a high exchange current density. Such conditions are met for alloys with a rhenium content of 60–70 at%.

## Author contributions

This manuscript was written through contributions of all the authors. All the authors have given approval to the final version of the manuscript.

## Conflicts of interest

There are no conflicts to declare.

## Acknowledgements

Our group acknowledges to financial support from the National Academy of Sciences of Ukraine within the state budget theme “Finishing processing of materials in order to give them unique functional properties” 0123U100650.

## Notes and references

- 1 A. Vargas-Uscategui, E. Mosquera and L. Cifuentes, *Electrochim. Acta*, 2013, **109**, 283–290.
- 2 Yu. S. Yapontseva, T. V. Maltseva, V. S. Kublanovsky, O. A. Vyshnevskiy and Yu. N. Troshchenkov, *Int. J. Refract. Met. Hard Mater.*, 2021, **96**, 105469.
- 3 N. Eliaz and E. Gileadi, in *Induced codeposition of alloys of tungsten, molybdenum and rhenium with transition metals*, ed C. G. Vayenas, R. E. White, M. E. Gamboa-



- Aldeco, *Modern Aspects of Electrochemistry*. 42, Springer, New York. 2008, vol. 191, Ch. 4.
- 4 Q. Huang and T. W. Lyons, *Electrochem. Commun.*, 2018, **93**, 53–56.
  - 5 S. De, W. D. Sides, T. Brusuelas and Q. Huang, *J. Electroanal. Chem.*, 2020, **860**, 113889.
  - 6 B. Malekpouri, K. Ahammed and Q. Huang, *J. Alloys Compd.*, 2022, **912**, 165077.
  - 7 A. Naor, N. Eliaz and E. Gileadi, *Electrochim. Acta*, 2009, **54**(25), 6028–6035.
  - 8 O. Bersirova and V. Kublanovsky, *Mater. Sci.*, 2019, **54**, 506–511.
  - 9 J. Niedbała, M. Popczyk, D. Kopyto, A. S. Swinarew and I. Matuła, *Rev. Adv. Mater. Sci.*, 2021, **60**(1), 784–793, DOI: [10.1515/rams-2021-0058](https://doi.org/10.1515/rams-2021-0058).
  - 10 Y. Yapontseva, V. Kublanovsky and O. Vyshnevskiy, *J. Alloys Compd.*, 2018, **766**, 894–901.
  - 11 Stability constants of metal-ion complexes. Section B: Organic Ligands, ed Douglas D. Perrin, *IUPAC Chemical Data Series 22*, Pergamon Press, Exter, 1983.
  - 12 M. Kohlickova, V. Jedinakova-Krizova and R. Konirova, *J. Radioanal. Nucl. Chem.*, 1999, **242**, 545.
  - 13 A. Subramania, A. R. Sathya Priya and V. S. Muralidharan, *Int. J. Hydrogen Energy*, 2007, **32**, 2843–2847.
  - 14 A. Krohn and Th. M. Brown, *J. Electrochem. Soc.*, 1961, **108**, 60.
  - 15 A. Krasikov and V. Krasikov, *Russ. J. Appl. Chem.*, 2009, **82**, 846–850.
  - 16 E. J. Podlaha and D. Landolt, *J. Electrochem. Soc.*, 1997, **144**(5), 1672–1680.
  - 17 V. Nikitenko, Yu Yapontseva and V. Kublanovsky, *Ukr. Chem. J.*, 2022, **88**(4), 113–122, DOI: [10.33609/2708-129X.88.04.2022.113-122](https://doi.org/10.33609/2708-129X.88.04.2022.113-122).
  - 18 I.O. Patsai Potentiostat-galvanostat MTech PGP-550F. <http://chem.lnu.edu.ua/mtech/devices.htm>.
  - 19 N. Kotsakis, C. P. Raptopoulou, V. Tangoulis, A. Terzis, J. Giapintzakis, T. Jakusch, T. Kiss and A. Salifoglou, *Inorg. Chem.*, 2003, **42**(1), 22–31.
  - 20 A. C. Frank and P. T. A. Sumodjo, *Electrochim. Acta*, 2014, **132**, 75–82.
  - 21 Y. Liu, Zh Li, Yi Wang and W. Wang, *Trans. Nonferrous Met. Soc. China*, 2014, **24**, 876–883.
  - 22 S. Kovaleva, I. Shabanova and A. Korshunov, *Izv. Tomsk. Politekh. Univ. Inz. Georesur.*, 2019, **330**(3), 163–174, DOI: [10.18799/24131830/2019/3/175](https://doi.org/10.18799/24131830/2019/3/175).
  - 23 V. Zhulikov and Yu Gamburg, *Russ. J. Electrochem.*, 2016, **52**, 847–857.
  - 24 T. Nenastina, M. Ved', N. Sakhnenko and V. Proskurina, *Adv. Surf. Appl. Electrochem.*, 2021, **57**(1), 59–66.
  - 25 Y. Yapontseva, T. Maltseva and V. Kublanovsky, *et al.*, *J. Mater. Res.*, 2022, **37**(13), 2216–2224.
  - 26 S. S. Grabchikov and A. M. Yaskovich, *Russ. Metall.*, 2006, **2006**, 56–60.
  - 27 P. Bacal, M. Donten and Z. Stojek, *Electrochim. Acta*, 2017, **241**, 449–458.
  - 28 J. García-Torres, E. Gómez and E. Vallés, *J. Appl. Electrochem.*, 2009, **39**, 233–240.
  - 29 H. L. S. Santos, P. G. Corradini, M. Medina and L. H. Mascaro, *Int. J. Hydrogen Energy*, 2020, **45**(58), 33586–33597.
  - 30 A. C. Thenuwara, L. Dheer, N. H. Attanayake, Q. Yan, U. V. Waghmare and D. R. Strongin, *ChemCatChem*, 2018, **10**(21), 4832–4837.
  - 31 V. Kuznetsov, A. Kalinkina and T. Pshenichkina, *et al.*, *Russ. J. Electrochem.*, 2008, **44**, 1350–1358.
  - 32 E. Vernickaite, N. Tsyntsaru, K. Sobczak and H. Cesiulis, *Electrochim. Acta*, 2019, **318**, 597–606.
  - 33 T. Nenastina, M. Ved, M. Sakhnenko, V. Proskurina and S. Zyubanova, *Mater. Sci.*, 2021, **56**(5), 634–641.
  - 34 N. M. N. Rozlin and A. M. Alfantazi, *Appl. Electrochem.*, 2013, **43**, 721–734.
  - 35 J. B. Lambert, *Refractory Metals and Alloys. Properties and Selection: Nonferrous Alloys and Special-Purpose Materials*, ASM HANDBOOK, 1990, Vol. 2, DOI: [10.31399/asm.hb.v02.9781627081627](https://doi.org/10.31399/asm.hb.v02.9781627081627).

